



# The Bromodomain Protein Brd4 Insulates Chromatin from DNA Damage Signaling

## Citation

Floyd, S. R., M. E. Pacold, Q. Huang, S. M. Clarke, F. C. Lam, I. G. Cannell, B. D. Bryson, et al. 2013. "The Bromodomain Protein Brd4 Insulates Chromatin from DNA Damage Signaling." *Nature* 498 [7453]: 246-250. doi:10.1038/nature12147. <http://dx.doi.org/10.1038/nature12147>.

## Published Version

doi:10.1038/nature12147

## Permanent link

<http://nrs.harvard.edu/urn-3:HUL.InstRepos:11879319>

## Terms of Use

This article was downloaded from Harvard University's DASH repository, and is made available under the terms and conditions applicable to Other Posted Material, as set forth at <http://nrs.harvard.edu/urn-3:HUL.InstRepos:dash.current.terms-of-use#LAA>

## Share Your Story

The Harvard community has made this article openly available.  
Please share how this access benefits you. [Submit a story](#).

[Accessibility](#)

Published in final edited form as:

*Nature*. 2013 June 13; 498(7453): 246–250. doi:10.1038/nature12147.

## The Bromodomain Protein Brd4 Insulates Chromatin from DNA Damage Signaling

Scott R. Floyd<sup>1,4</sup>, Michael E. Pacold<sup>1,8,9</sup>, Qiuying Huang<sup>1</sup>, Scott M. Clarke<sup>1</sup>, Fred C. Lam<sup>1</sup>, Ian G. Cannell<sup>1</sup>, Bryan D. Bryson<sup>1</sup>, Jonathan Rameseder<sup>1</sup>, Michael J. Lee<sup>1</sup>, Emily J. Blake<sup>1</sup>, Anna Fydrych<sup>1</sup>, Richard Ho<sup>1</sup>, Benjamin A. Greenberger<sup>1</sup>, Grace C. Chen<sup>1</sup>, Amanda Maffa<sup>1</sup>, Amanda M. Del Rosario<sup>1</sup>, David E. Root<sup>6</sup>, Anne E. Carpenter<sup>6</sup>, William C. Hahn<sup>6,7</sup>, David M. Sabatini<sup>6,9</sup>, Clark C. Chen<sup>5,7</sup>, Forest M. White<sup>1,3</sup>, James E. Bradner<sup>6,7</sup>, and Michael B. Yaffe<sup>1,2,3,5,6,†</sup>

<sup>1</sup>Koch Institute for Integrative Cancer Research, Massachusetts Institute of Technology, Cambridge, MA 02139, USA

<sup>2</sup>Dept. of Biology, Massachusetts Institute of Technology, Cambridge, MA 02139, USA

<sup>3</sup>Dept. of Biological Engineering, Massachusetts Institute of Technology, Cambridge, MA 02139, USA

<sup>4</sup>Dept. of Radiation Oncology, Beth Israel Deaconess Medical Center, Boston, MA 02215, USA

<sup>5</sup>Dept. of Surgery, Beth Israel Deaconess Medical Center, Boston, MA 02215, USA

<sup>6</sup>Broad Institute of Harvard & MIT, Cambridge, MA 02142, USA

<sup>7</sup>Dept. of Medical Oncology, Dana-Farber Cancer Institute, Boston, MA 02215, USA

<sup>8</sup>Dept. of Radiation Oncology, Dana-Farber Cancer Institute, Boston, MA 02215, USA

<sup>9</sup>Whitehead Institute, Cambridge, MA 02139 USA

DNA damage activates a signaling network that blocks cell cycle progression, recruits DNA repair factors, and/or triggers senescence or programmed cell death.<sup>1</sup> Alterations in chromatin structure are implicated in the initiation and propagation of the DNA damage response (DDR).<sup>2</sup> We further investigated the role of chromatin structure in the DDR by monitoring ionizing radiation-induced signaling and response events with a high-content multiplex RNAi screen of chromatin modifying and interacting genes. We discovered that an isoform of Brd4, a bromodomain and extra-terminal (BET) family member, functions as an endogenous inhibitor of DDR signaling by recruiting the condensin II chromatin

<sup>†</sup>Correspondence and requests for materials should be addressed to M.B.Y. (myaffe@mit.edu).

**Author Contributions** S.R.F. and M.B.Y. designed the study, supervised the experiments, analysed the data, and wrote the manuscript. D.E.R., W.C.H., and D.M.S. were involved in the design and preparation of the lentiviral shRNA library. S.R.F., MEP, and EB performed the image-based high content screen and initial analysis. A.E.C. aided in digital image analysis. S.R.F., Q.H., S.M.C., F.C.L., I.G.C., M.J.L., A.F., R.H., B.A.G., G.C.C., and A.M. performed biochemical, cell biological and molecular biological experiments. B.D.B., A.M.D., and F.M.W. performed mass spectrometry experiments and analysis. J.R. performed bioinformatics analysis. J.E.B. contributed JQ1 compounds and cell lines. S.R.F. and M.B.Y. designed and supervised the experiments. C.C.C., J.E.B., and F.M.W. contributed to the intellectual development of the study and technical writing of the manuscript. All authors contributed in editing the manuscript.

The expression profiling Affymetrix u133 plus dataset is deposited at the NCBI Gene Expression Omnibus (GEO) accession number GSE30700.

Reprints and permissions information is available at [www.nature.com/reprints](http://www.nature.com/reprints).

The authors declare no competing financial interests.

Readers are welcome to comment on the online version of this article at [www.nature.com/nature](http://www.nature.com/nature).

remodeling complex to acetylated histones via bromodomain interactions. Loss of this isoform results in relaxed chromatin structure, rapid cell cycle checkpoint recovery and enhanced survival post-irradiation, while functional gain of this isoform compacted chromatin, attenuated DDR signaling, and enhanced radiation-induced lethality. These data implicate Brd4, previously known for its role in transcriptional control, as an insulator of chromatin that can modulate the signaling response to DNA damage.

Detection and repair of damaged DNA is integral for cell survival and accurate transmission of genetic information to progeny. Defects in the DDR contribute to oncogenesis and genomic instability in tumors<sup>3,4</sup> and render tumor cells sensitive to DNA-damaging cancer therapy.<sup>5</sup> Early signaling events that trigger and transduce the DDR occur in the context of chromatin, and it is likely that modulation of chromatin structure plays a role in DDR signaling.<sup>2</sup> Histone proteins are known targets of DDR post-translational modification,<sup>2,6</sup> but a detailed understanding of the role of chromatin modulation in the DDR is lacking.

To explore the role of chromatin modulation in the DDR, we developed a high-throughput, high-content quantitative microscopy assay multiplexed for early and late DDR endpoints, and applied this to an RNAi library focused on proteins that interact with and modify chromatin (see full Methods).<sup>7</sup> For each time point, cells were co-stained with  $\gamma$ H2AX antibodies to measure early signaling events in the DDR; Hoechst 33342 to monitor cell cycle progression; and phospho-histone H3 (pHH3) to measure mitotic entry. At the latest timepoint, cleaved caspase-3 (CC3) was substituted for pHH3 to measure apoptotic cell death. The screening assay was validated with small molecule inhibitors of DDR signaling as well as RNAi directed against known components of the DDR pathway (Supplementary Figs. 1–4).

The most pronounced increase in  $\gamma$ H2AX foci number, size and intensity following IR was observed at 1 and 6 hr after knockdown of Brd4; this remained elevated at 24 hr (Fig. 1a,b, Supplementary Fig. 4). Eight hairpins directed against Brd4 showed this effect, making off-target effects unlikely (Fig. 1a, Supplementary Fig. 4). Neither Brd4 knockdown in the absence of irradiation (Fig. 1b) nor knockdown of other bromodomain-containing proteins (Figs. 1b, Supplementary Fig. 4) significantly altered  $\gamma$ H2AX. Increased IR-induced  $\gamma$ H2AX after Brd4 loss was further confirmed using siRNA oligonucleotides targeting additional independent Brd4 sequences (Fig. 1f, Supplementary Fig. 5).

Brd4 encodes 3 splice isoforms (A, B and C in Fig. 1c). Each isoform contains two N-terminal bromodomains (BD1 and BD2) that bind acetylated lysine, and an extra-terminal (ET) domain recently reported to interact with several chromatin-binding proteins.<sup>9</sup> The A isoform contains a C-terminal domain (CTD) that functions as a transcriptional co-activator with the pTEFb complex.<sup>10,11</sup> This region is notably absent in the B and C isoforms, and in the B isoform, it is replaced with a divergent short 75 amino acid segment. All three Brd4 isoforms are expressed in U2OS cells, and the shRNAs used in our initial screen targeted all three isoforms (Supplementary Table 1). We confirmed that a single distinct siRNA that was active against all Brd4 isoforms replicated the Brd4 loss-of-function phenotype of elevated IR-induced  $\gamma$ H2AX (Supplementary Fig. 5).

To establish the relative effects of the isoforms on the DDR, we performed gain-of-function experiments. Overexpression of Brd4 isoform B most potently suppressed IR-induced  $\gamma$ H2AX foci (Fig. 1d). We designed isoform-specific siRNAs to selectively reduce expression of isoform A or B mRNA (Fig. 1e) and protein (Supplementary Fig. 5); selective targeting of isoform C was not technically possible owing to complete coding sequence overlap with isoforms A and C. We observed that selective depletion of Brd4 isoform B, but

not isoform A, increased H2AX phosphorylation over a wide range of ionizing radiation doses (Fig. 1f).

To investigate whether elevated  $\gamma$ H2AX levels observed in Brd4-deficient cells resulted from increased production of IR-induced DNA double-strand breaks (DSBs) or from faulty DSB repair, we used pulsed-field gel electrophoresis to quantify DSBs in control and Brd4 knockdown cells. As shown in Fig. 2a, Brd4 knockdown had minimal effects on the generation and repair kinetics of DSBs. These observations, together with our finding that individual  $\gamma$ H2AX foci were larger and more intense in irradiated Brd4 knockdown cells (Fig. 1b, Supplementary Fig. 4, Supplementary Tables 1,2), suggest that there is enhanced signaling from damaged DNA in the absence of Brd4, rather than an increase in the amount of damage or repair deficiency.

Changes in overall chromatin structure can affect H2AX phosphorylation, likely by controlling the accessibility of signaling molecules to DNA damage sites.<sup>12,13</sup> Interestingly,  $\gamma$ H2AX foci form more readily in “open” areas of euchromatin<sup>14</sup>, histone acetylation has been linked to the “open” chromatin state, and histone deacetylase inhibitors are known to increase H2AX phosphorylation.<sup>15</sup> We speculated that a bromodomain protein could influence H2AX phosphorylation via interaction with acetylated histones and effects on global chromatin structure, and therefore performed micrococcal nuclease susceptibility experiments. Knockdown of Brd4 isoform B increased digestion by micrococcal nuclease, indicating a more “open” overall chromatin structure, while knockdown of isoform A had minimal effects (Fig. 2b). Furthermore, we observed that cells transfected with Brd4 isoform B showed a distinct nuclear DAPI staining pattern, indicating a change in chromatin structure (Fig. 2c). As shown in Fig. 2d,e, quantification of the nuclear staining texture revealed a more heterogeneous DAPI intensity pattern, and significantly lower pixel-to-pixel correlation of DAPI staining in cells overexpressing isoform B, indicative of isoform B-mediated alterations in global chromatin structure. Expression of isoform A had no effect on DAPI staining, while overexpression of isoform C had smaller effects than those observed with isoform B.

Our finding that Brd4 isoform B expression affects global chromatin structure and attenuates H2AX phosphorylation in response to DNA damage led us to investigate the subcellular localization of isoform B in response to ionizing radiation. Immunofluorescence experiments showed that ionizing radiation did not grossly alter Brd4 isoform B nuclear localization, which tightly mirrored DNA patterns revealed by DAPI staining (Supplementary Fig. 6a). Interestingly, subcellular fractionation of U2OS cells and extraction of chromatin bound proteins demonstrated that irradiation caused enhanced isoform B association with the high salt-extractable chromatin fraction (Supplementary Fig. 6b,c), indicating increased association of isoform B with chromatin after DNA damage.

Bromodomains recognize epigenetic marks on chromatin via binding to acetyl-lysine.<sup>16</sup> We therefore tested the contribution of Brd4 bromodomain interactions to alterations in  $\gamma$ H2AX phosphorylation using JQ1, a small molecule inhibitor of BET bromodomains.<sup>17</sup> Only the active enantiomer of JQ1 caused increased H2AX phosphorylation following irradiation in U2OS cells (Fig. 2f), similar to the effects observed following Brd4 isoform-B specific knockdown. Furthermore, JQ1 treatment or Brd4 isoform B knock-down did not significantly alter total histone levels or levels of histone acetylation (Supplementary Figs. 7,8). Interestingly, overexpression of Brd4 isoform B led to alteration in the nuclear staining pattern of acetyl-lysine, closely mirroring the DAPI staining pattern induced by expression of isoform B (Supplementary Fig. 7b).

The concentration of JQ1 that we used (250 nM) is consistent with the reported *in vitro* IC<sub>50</sub> for Brd4 bromodomains 1 (BD1, 77 nM) and 2 (BD2, 33 nM).<sup>17</sup> To directly evaluate the role of each bromodomain in isoform B, we performed gain-of-function experiments using wild-type Brd4 in the absence or presence of JQ1, or constructs harboring mutations that abrogate acetyl lysine binding by BD1 or BD2. Mutations in BD1, or addition of the active enantiomer of JQ1, potently reversed the  $\gamma$ H2AX-suppressive effects of isoform B expression (Fig. 2g). Notably, mutations that abrogate BD1 binding to acetyl-lysine also rescued the IR-induced cell death phenotype observed with Brd4 isoform B gain-of-function (see below), implicating BD1 in the mechanism of DNA damage inhibition (Fig. 4b).

To further probe the role of lysine acetylation on  $\gamma$ H2AX-Brd4 effects, we examined the combined effects of histone deacetylase inhibitors and Brd4 knockdown. We found that when Brd4 isoform B knockdown was combined with exposure to 50 nM LBH589, an inhibitor of histone deacetylases (HDAC) 1–3 and 6,<sup>18</sup> H2AX phosphorylation was enhanced to a greater extent than with either treatment alone (Supplementary Fig. 9). This effect could be observed even in unirradiated cells, although the total level of H2AX phosphorylation remained lower than that seen in irradiated cells. Taken together, these findings indicate that Brd4 isoform B binding to acetylated regions of chromatin alters chromatin structure and limits H2AX phosphorylation.

Brd4 also has a defined role in transcriptional modulation, largely via interactions of isoform A with the pTEFb transcriptional complex.<sup>10,11</sup> To investigate the contribution of Brd4-driven transcriptional changes to the suppression of DNA damage signaling, we profiled mRNA expression patterns of cells stably expressing control or Brd4 shRNAs. Only one DDR-associated transcript, CHEK2, showed a differential expression change of 2-fold or more (Supplementary Fig. 10a). Importantly, transient Brd4 knockdowns with siRNA, or short-term inhibition with JQ1, both of which increased  $\gamma$ H2AX foci formation after irradiation (Supplementary Fig. 5a, Fig. 2f), caused no change in CHEK2 mRNA levels (Supplementary Fig. 10b,c), and neither long-term nor short term Brd4 knockdown affected the protein levels of several DDR molecules, including Chk2 (Supplementary Fig. 10d). Moreover, the suppression of DDR signaling by Brd4 isoform B overexpression was insensitive to transcription and translation inhibition with  $\alpha$ -amanitin and cycloheximide, respectively (Supplementary Fig. 11).

As interactions between Brd4 and other protein complexes involved in modulating chromatin structure were likely to be responsible for the DDR effects we observed, we identified proteins co-immunoprecipitated with isoform B after DNA damage using mass spectrometry (Fig. 3a, Supplementary Fig. 12). From two independent experiments, we obtained a common set of 57 interacting proteins (Supplementary Tables 3,4). Since the DDR-relevant Brd4-binding proteins presumably function in the same pathway as Brd4, we reasoned that loss of these proteins should show a phenotype similar to Brd4 loss-of-function. We therefore used our existing HCS screen data to create a list of the top quartile of genes ranked by increased  $\gamma$ H2AX foci intensity, number, and size at 1 and 6 hr following irradiation (Fig. 3b). The overlap of this list with the list of isoform B interacting proteins revealed two members of the condensin II complex, SMC2 and CAPD3 (Fig. 3c,d). This finding was intriguing as the condensin II complex has a known role in chromatin compaction in both mitotic and interphase cells, and has been linked to DNA damage repair.<sup>19</sup> We performed immunoprecipitation experiments after DNA damage, and found that the SMC2 and SMC4 components of the condensin II complex co-immunoprecipitated with Brd4 isoform B, while Brd4 isoform A had minimal co-association (Fig. 3e). To verify the role of this interaction on the  $\gamma$ H2AX effects we observed, we performed combined isoform B and SMC2 knockdown and assayed H2AX phosphorylation 24 hr after siRNA transfection, when knockdown of each protein is sub-maximal. We found that H2AX

phosphorylation was enhanced with combined knockdown over knockdown of either protein alone (Fig. 3f,g). Furthermore, in cells overexpressing isoform B, SMC2 knockdown could abrogate the suppressive effects of Brd4 on  $\gamma$ H2AX, demonstrating a functional interaction between isoform B and the condensin II complex in modulating  $\gamma$ H2AX (Fig. 3h,j). Finally, we noted that the effects of isoform B on the DAPI staining pattern of chromatin were abrogated by co-transfection of SMC2 siRNA, indicating that the Brd4-condensin II interaction is involved in chromatin structure alterations (Fig. 3i).

We next investigated isoform B effects on other components of the DDR. We found that isoform B gain-of-function inhibited IR-induced foci formation of several additional known DDR signaling components including 53BP1, phosphorylated ATM, and multiple DDR signaling molecules containing the phospho-SQ DDR kinase substrate motif (Fig. 4a). In addition, overexpression of isoform B resulted in increased cell death following irradiation, an effect that was significantly diminished by mutation of BD1 (Fig. 4b). The cell death observed in Brd4 isoform B overexpressing cells appears to result from mitotic catastrophe, consistent with a loss of DDR signaling that results in failed cell cycle arrest (Supplementary Fig. 13). We also investigated the effect of isoform B knockdown on DDR-induced cell cycle arrest and survival. Interestingly, isoform B loss-of-function allowed increased cell survival with more rapid and efficient recovery from cell-cycle arrest after irradiation, complementing the inverse findings observed with isoform B gain-of-function (Fig. 4c,d).

Given the effects of Brd4 isoform B on IR-induced DDR signaling and survival, we hypothesized that isoform B might have a role in tumor responses to irradiation. We screened a panel of established cell lines from several human tumor types commonly treated with radiotherapy for  $\gamma$ H2AX effects using the JQ1 inhibitor. Several cell types showed increased IR-induced H2AX phosphorylation with JQ1 treatment, including breast, prostate, and particularly glioma cancer cell lines (Fig. 4e). Just as we had observed with U2OS cells, irradiation had the expected killing effect on DMSO-treated glioma cells, however, this killing effect was dramatically reduced in JQ1-treated glioma cells, consistent with our finding of increased DDR signaling and radioresistance with decreased Brd4 function (Fig. 4f). Conversely, overexpression of Brd4 isoform B in glioma cells inhibited H2AX phosphorylation, consistent with decreased DDR signaling upon Brd4 gain-of-function (Supplementary Fig. 14).

We conclude that structural alterations in chromatin mediated by Brd4 acetyl lysine binding function to attenuate the DNA damage signaling response to IR. These effects on DDR signaling are consistent with the induction of a chromatin structure that is inhibitory to the formation of  $\gamma$ H2AX in the case of higher levels of Brd4 isoform B expression, or a more “open” chromatin structure that facilitates  $\gamma$ H2AX foci formation when Brd4 expression is reduced, or following pharmacological inhibition of bromodomain binding (shown schematically in Fig. 4g).

Our data indicate that Brd4 affects DDR signaling via mechanisms distinct from known transcriptional interactions with the P-TEFb transcriptional complex. The relevant Brd4 isoform that modulates the DDR, isoform B, lacks the pTEFb-interacting region. In addition, chemical inhibition of transcription/translation had no effect on the ability of Brd4 to suppress DDR-induced  $\gamma$ H2AX. This finding is in line with the recent identification of other chromatin-interacting proteins such as KAP-1 and Brg1 that have roles in DNA damage signaling that do not seem to arise directly from transcriptional activity that these molecules also possess.<sup>13,20</sup> Rather, the enhancement of multiple parameters of  $\gamma$ H2AX foci following Brd4 knockdown, including their size, and intensity, in addition to their number, point to a role for Brd4 in limiting the propagation of DDR signaling following IR. This effect seems



to involve the recruitment of a chromatin-condensing complex to sites of acetylation, a novel role for Brd4. In agreement with this, overexpression of Brd4 even in the absence of damage resulted in alterations of chromatin structure and nuclear acetylation patterns, consistent with a model of Brd4 isoform B binding to and occluding acetyl-lysine sites on chromatin and recruiting chromatin compaction machinery. These findings implicate bromodomain-mediated interactions in modulating specific chromatin structures that inhibit the propagation of DDR signaling in chromatin,<sup>12,15</sup> and indicate that Brd4 isoform B alters the threshold response of  $\gamma$ H2AX to DNA damage.

## Methods

### Antibodies and stains

Mouse monoclonal antibodies against  $\gamma$ H2AX were from Upstate/Millipore (cat. #05636), Actin (Sigma, cat. #A5441), phospho-ATM Serine 1981 (Rockland, cat. #200-301-400), FLAG (Sigma, cat. #F3165), ornithine decarboxylase (Abcam, cat. #ab66067), RAD50 (GeneTex cat. #GTX70228), NBS1 (Abcam cat. #ab49958), MDC1 (Novus cat. #NB100-396), and Lamin (Millipore cat. #05-714). Rabbit polyclonal and monoclonal antibodies against Brd4 were from Abcam (cat. #Ab46199) and Pan-Brd4 from Sigma (cat. #AV39076), 53BP1 (Novus cat. #NB100-304), CHEK2 (Cell Signaling Technologies cat. #2662), total H2AX (Abcam, cat. #ab11175), phospho-SQ (Cell Signaling Technologies, cat. #2851), MRE11 (Novus cat. #NB100-142), cleaved caspase 3 (Cell Signaling Technologies, cat. #9664), SMC2 (Cell Signaling Technologies cat. #5329), SMC4 (Cell Signaling Technologies cat. #5547), phospho-histone H3 (Upstate/Millipore cat. #06570 and BD/Pharmingen cat. #559565). DNA stains were Hoechst 33342 (Invitrogen cat. #H1399) propidium iodide (Invitrogen cat. #P1304MP) and ethidium bromide (Invitrogen cat. #15585011). Fluorescent antibodies were from Invitrogen: goat anti-rabbit and goat anti-mouse Alexa 488, 555 and 647 cat. #A11001, A21422, A21235, A21238, A21428, and A21244).

### Small molecule inhibitors

Brd4 bromodomain inhibitor (+)JQ1 and its inactive enantiomer (–)JQ1 were synthesized as described (**1**) and were used at 250 nM.  $\alpha$ -amanitin (cat. #A2263) and cycloheximide (cat. #C4859) were from Sigma and were used at concentrations as indicated ( $\alpha$ -amanitin: 1–16  $\mu$ M, cycloheximide 35–560  $\mu$ M). UCN01 was from Sigma (cat. #U6508) and was used at concentrations of 0.003–10  $\mu$ M. Caffeine was from Sigma (cat. #C0750) and was used at concentrations 10–25 mM. LBH589 was gift from Dr. James Bradner, Dana Farber Cancer Institute, Boston, MA, USA).

### RNAi library

shRNA was applied to cells using a high-titer arrayed lenti-viral library maintained in the pLKO\_TRC001 vector as described (MOFFET, ROOT 2006).

### Image-based screens

For both shRNA and small molecule screens, human U2OS osteosarcoma cells (ATCC HTB-96) were grown in DMEM + Pen/Strep + 10% v/v FBS (complete media) at 37°C in a 5% CO<sub>2</sub> atmosphere. All screens were carried out at passage 10–15. Cells were tested for mycoplasma by PCR prior to seeding and infection. U2OS cells were seeded with a MicroFill (Biotek) in 384-well black, clear bottom plates (Greiner) at a density of 300 (shRNA) cells/well in 50  $\mu$ L of media, and allowed to attach overnight at 37°C in a 5% CO<sub>2</sub> atmosphere. For shRNA screens, the media was exchanged the following day to complete media with 8  $\mu$ g/mL polybrene using a JANUS workstation (PerkinElmer). Virus infection

was carried out on an EP3 workstation (PerkinElmer) with 1.5  $\mu$ L of hightiter retrovirus. All plates had two wells infected with 1.5  $\mu$ L of control virus with shRNA directed against H2AX. Plates were centrifuged in a swinging-bucket rotor at 2250 rpm for 30 minutes following infection and returned to the incubator overnight. The plates were then selected with 2.5  $\mu$ g/mL puromycin for 48 hours, and allowed to proliferate in complete media for another 48 hr, with media exchanges carried out on the JANUS or RapidPlate (Qiagen) liquid handling workstations. Eight wells in each plate were not selected with puromycin. For small molecule testing, cells were plated at 500 cells/well in 384-well plates. The day after plating, small molecules at different concentrations in 100 nL DMSO were pin transferred to cells with a CyBio robot, and cells were propagated for 16 hr. For both small molecule and shRNA screens, four plates were created in replicate for the timepoints outlined below. Four wells were left untreated in each plate, and received 25 mM caffeine in complete media 1 hr prior to irradiation. All plates were treated with 10 Gy of 667 keV X-rays from a  $^{137}\text{Cs}$  source in a Gammacell irradiator (Atomic Energy of Canada, Ltd). A 0 hr control plate was not irradiated. The plates were returned to the incubator and fixed with 4.4% w/v paraformaldehyde in phosphate-buffered saline (PBS) at 1, 6, and 24 hr post-irradiation. Plates were stored in PBS at 4°C prior to staining. Fixed plates were washed 3 times with PBS and blocked with 24  $\mu$ L of GSDB (0.15% goat serum, 8.33% goat serum, 120 mM sodium phosphate, 225 mM NaCl) for 30 minutes. The 0, 1, and 6 hr plates were incubated with 1:300 dilutions in GSDB of primary mouse monoclonal anti- $\gamma$ H2AX (Ser 139), and rabbit polyclonal anti-pHH3 antibody. For the 24 hr plates, we substituted 1:300 rabbit polyclonal anti-cleaved Caspase 3 for the pHH3 antibody. All plates were incubated overnight at 4°C, washed, and stained with a secondary antibody mix containing 10  $\mu$ g/mL Hoescht 33342, 1:300 goat anti-mouse polyclonal-Alexa Fluor 488, and goat anti-rabbit polyclonal-Alexa Fluor 555 in GSDB. After a second overnight incubation at 4°C, the plates were washed 3 times in PBS and stored in 50  $\mu$ L/well 50  $\mu$ M Trilox (Sigma) in PBS at 4°C.

### Imaging and image analysis

Plates were allowed to equilibrate to room temperature for 30 min and imaged on a Cellomics ArrayScan VTI automated microscope with a 20x objective. The acquisition parameters were the same for each shRNA or chemical library. Six fields per well were imaged, with three channels/field (DAPI, fluorescein and rhodamine) for a total of 18 acquired images per well. Images were segmented and analyzed with CellProfiler cell image analysis software (Carpenter et al., Genome Biology 2006, 7, R100). The imaging pipeline used to segment the images is available on request. Cell morphology and intensity data were acquired on a per image and per cell basis, and exported into a MySQL database. The data were visualized with SpotFire (TIBCO) and CellProfiler Analyst (2, 3).

### Immunofluorescence microscopy

U2OS cells were plated on #1 glass coverslips (VWR) and were cultured in DMEM + Pen/Strep + 10% v/v FBS (complete media) at 37°C in a 5% CO<sub>2</sub> atmosphere, then exposed to 10 Gy Ionizing radiation from a  $^{137}\text{Cs}$  source in a Gammacell irradiator (Atomic Energy of Canada, Ltd). fixed in methanol, and processed for immunofluorescence using the antibodies indicated above. Images were captured on a Zeiss Axiophot II microscope with a Hamamatsu CCD camera and processed with OpenLab/Volocity software. Quantitative image analysis was accomplished using CellProfiler ([www.CellProfiler.org](http://rsb.info.nih.gov/nihimageJ)) or ImageJ software (<http://rsb.info.nih.gov/nihimageJ>).

### RT-PCR

Total RNA was extracted from 106 U2OS cells expressing either control or Brd4-directed shRNA, or from 1 mg tumor tissue (as described below) that had been flash frozen in liquid



nitrogen with a RNeasy kit (Qiagen). cDNA was generated with oligo dT primers with SuperScript reverse transcriptase (Invitrogen) according to manufacturer's instructions. These cDNAs were used as templates for linear-range PCR amplification or quantitative real-time PCR with SYBR green master mix on an Applied Biosystems 7500 with the following primers: forward- 5' CTC CTC CTA AAA AGA CGA AGA-3', and reverse (pan-Brd4 isoform) 5'-TTC GGA GTC TTC GCT GTC AGA GGA G-3', (Brd4 isoform A) 5'-GCC CCT TCT TTT TTG ACT TCG GAG C-3', (Brd4 isoform B) 5'-GCC CTG GGG ACA CGA AGT CTC CAC T-3', (Brd4 isoform C) 5'-CCG TTT TAT TAA GAG TCC GTG TCC A-3', (CHEK2) forward 5'-ACAGATAAATAC CGAACATACAGC-3' and reverse 5'-GACGGCGTTTTCCTTTCCTACAA-3', and using (GAPDH) primers forward 5'-GATGCCCTGGAGGAAGTGCT-3' and reverse 5'-AGCAGGCACAA CACCACGTT-3' as control for normalization.

### Expression profiling and analysis

Total RNA was harvested from stable U2OS cells expressing Brd4 or control shRNA using RNeasy (Qiagen), labeled and analyzed on the Affymetrix U133 Plus 2.0 array. Unsupervised clustering of expression data was performed using the R package pvclst. LIMMA (4) was used to identify significant changes in expression between Brd4 knockdown and control cells. Data were deposited in the U.S. National Institutes of Health Gene Expression Omnibus (GEO). (<http://www.ncbi.nlm.nih.gov/geo/query/acc.cgi?acc=GSE30700>)

### Subcellular fractionation

U2OS cells expressing Flag-tagged Brd4 isoforms were lysed in hypotonic conditions (10 mM Hepes, 10 mM NaCl, 25 mM KCl, 1 mM MgCl<sub>2</sub>, 0.1 mM EDTA, pH 7.4 with protease inhibitors) and subjected to flash freezing in liquid nitrogen 1 hr after mock treatment or exposure to 10 Gy of ionizing radiation with a <sup>137</sup>Cs source in a Gammacell irradiator (Atomic Energy of Canada, Ltd). Cells were thawed at room temperature and spun down at 10,000 xg for 10 min. The supernatant was saved as the *cytoplasmic fraction* and concentrated down using trichloroacetic acid precipitation and reconstituted in 2x Laemmli buffer. The pellet was resuspended in high salt buffer (20 mM Hepes, 0.5 mM DTT, 1.5 mM MgCl<sub>2</sub>, 0.1% Triton X-100, 1 M NaCl, pH 7.4 with protease inhibitors) and left on ice for 30 min followed by a high-speed spin at 100,000 xg for 30 min. The supernatant was saved as the *high salt fraction* and concentrated down using trichloroacetic acid precipitation and reconstituted in 2x Laemmli buffer. Sulfuric acid (0.4 N) was added to the high-speed pellet and left on ice for 30 min, followed by a high-speed spin at 14,000 xg for 10 min. The supernatant was saved as the *acid fraction* and concentrated down using trichloroacetic acid precipitation and reconstituted in 2x Laemmli buffer.

### Western blotting and Immunoprecipitation

Cells were treated with 10 Gy ionizing radiation with a <sup>137</sup>Cs source in a Gammacell irradiator (Atomic Energy of Canada, Ltd). For whole cell lysates, cells were trypsinized and lysed in LB (4% SDS, 120 mM Tris, pH 6.8) with protease and phosphatase inhibitors (Complete mini EDTA-free and PhosSTOP, Roche Applied Science). For chromatin isolation, cells were trypsinized, resuspended in low salt buffer (LSB: 10 mM Hepes 10 mM NaCl, 25 mM KCl, 1.0 mM MgCl<sub>2</sub>, 0.1 mM EDTA, pH 7.4 + protease inhibitors, as above), flash-frozen in liquid N<sub>2</sub>, thawed, pelleted at 10,000 xg for 10 min, resuspended in high salt buffer (HSB: 20 mM Hepes, 1.0 M NaCl, 0.5 mM DTT, 1.5 mM MgCl<sub>2</sub>, 0.1% Triton X-100 + protease inhibitors) for 45 min on ice, pelleted at 100,000 xg for 30 min., and proteins from the supernatant were precipitated with trichloroacetic acid. For immunoprecipitation, U2OS cells expressing Flag-tagged Brd4 isoforms were lysed in low salt buffer (50 mM Tris

HCl, pH 7.4, 150 mM NaCl, 1 mM EDTA, 0.5% NP-40 with protease inhibitors) and subjected to flash freezing in liquid nitrogen 1 hr after mock treatment or irradiation. Cells were thawed at room temperature and spun down at 10,000 xg for 10 min. The supernatant was removed and saved as the *pre-IP cytoplasmic fraction*. The nuclear pellet was resuspended in low salt buffer, tip sonicated at 4°C (35% amplitude, pulse 5 sec on and off for 3 cycles), and spun down at 14,000 xg for 10 min. The supernatant was collected as starting material for IP using M2 Flag beads (Sigma Aldrich) overnight at 4°C. The beads were then spun down and the first supernatant saved as the *unbound fraction*. The beads were washed 5x with low salt buffer and proteins were solubilized in 2x Laemmli buffer and boiled at 95°C for 3 min prior to loading onto SDS PAGE. Samples were processed following SDS PAGE for gel band cutting and in gel tryptic digestion for mass spectrometry or western blotting to detect pulldown of the Condensin II complex (SMC2 and SMC4 proteins) with Brd4 isoforms. SDS-PAGE and Western blot was according to the methods of Laemmli and Towbin using either a Li-cor Odyssey ([www.licor.com](http://www.licor.com)) scanner or horseradish peroxidase-coupled secondary antibodies (Bio-Rad) and Western Lightning enhanced chemiluminescence (Perkin Elmer) for visualization of bands.

### Pulsed-field gel electrophoresis and micrococcal nuclease assay

For pulse field gel analysis, control and BRD4 knockdown cells were plated at  $1 \times 10^6$  cells per plate, exposed to 10 Gy IR with a  $^{137}\text{Cs}$  source in a Gammacell irradiator (Atomic Energy of Canada, Ltd) and harvested at 0.5, 1, 2, 3 and 5 hr. Cells were trypsinized, diluted to  $2 \times 10^6$  cells and embedded in agarose plugs. The agarose plugs were exposed to Proteinase K (1 mg/mL) in 500 mM EDTA, 1% N-lauryl Sarcosyl, pH 8.0, for 48 hr, washed 3 x 1 hr with TE buffer, loaded onto a 0.675% agarose gel, and separated under pulsed-field conditions with a Rotaphor 6.0 (Biometra, [www.biometra.com](http://www.biometra.com)). Nuclei from control and Brd4 knockdown cells were isolated by hypotonic lysis and micrococcal nuclease assays performed as described by Carey and Smale<sup>22</sup>.

### Flow cytometry

U2OS cells were plated and transiently transfected GFP transgenes or siRNA as indicated, exposed to varying doses of ionising radiation from a  $^{137}\text{Cs}$  Gammacell irradiator source (Atomic Energy of Canada, Ltd.), and harvested at varying times as indicated by fixation with 4% formaldehyde (cell death measurements) or directly extracted with 100% ethanol (cell cycle measurements), and processed for flow cytometry using the antibodies listed above. Data were analyzed using FlowJo ([www.flowjo.com](http://www.flowjo.com)) software.

### Colony formation assays

Control and BRD4 knockdown cells were exposed to the indicated doses of IR from a  $^{137}\text{Cs}$  source in a Gammacell irradiator (Atomic Energy of Canada, Ltd.), or left untreated, trypsinized, counted and re-plated using serial dilutions. Colonies were propagated to the 10–15 cell stage (3–7 days), stained with Wright stain (Sigma) and counted with CellProfiler software or by averaging counts of 10 fields from three independent observers using a dissection microscope to identify colonies of greater than 15 cells.

### Constructs, shRNA and siRNA, and transfection

Full-length constructs of Brd4-NUT (accession #AY166680.1), Brd4 Isoform A (accession # NM\_058243), B (accession #BC035266) and C (accession #NM\_014299.2) were cloned into pEGFP-C1 (Clontech) and pFLAG-CMV2 (Sigma) by PCR. Bromodomain mutations were introduced using quickchange (Stratagene) using PCR primers: 5'-AAA TTG TTA CAT CGC CAA CAA GCC TGG AGA TGA CGC AGT CTT AAT GGC AG-3' and 5'-CTG CCA TTA AGA CTG CGT CAT CTC CAG GCT TGT TGG CGA TGT AAC AAT

TT-3'. Cells were transfected using Fugene 6 (Roche) according to manufacturer's instructions. shRNA directed against Brd4 were from the TRC library (see Table S1), or created in the mir30-based pMLP vector (kind gift of Dr. Michael Hemann, MIT, Cambridge, MA, USA) with primer 5'-TGC TGT TGA CAG TGA GCG AAG ACA CA-3' for Brd4. U2OS cell lines stably expressing this shRNA or control hairpins (ineffective hairpins directed against human sequences of BAD and PUMA) were created using puromycin selection at 2 µg/mL. STEALTH siRNA against pan-isoform BRD4, SMC2, and control were purchased from Invitrogen. Custom Brd4 isoform-specific siRNA were synthesized from Dharmacon using the sequences: Isoform A specific 5'-GGG AGA AAG AGG AGC GUG AUU-3' and Isoform B specific 5'-GCA CCA GUG GAG ACU UCG UUU-3'. siRNA against SMC2 was from Dharmacon. For siRNA experiments, cells were transfected with Lipofectamine RNAiMax (Invitrogen) according to manufacturer's instructions.

### Mass spectrometry

Proteins from the Brd4 co-immunoprecipitation were examined after sodium dodecyl sulfate-polyacrylamide gel electrophoresis (SDS-PAGE) by staining with Coomassie Blue. Gel bands were excised, de-stained and processed for digestion with trypsin (Promega; 12.5 ng/µl in 50 mM ammonium bicarbonate, pH 8.9). Peptides were loaded directly onto a column packed with C18 beads. The column was placed in-line with a tapered electrospray column packed with C18 beads on a Orbitrap XL mass spectrometer (Thermo Scientific). Peptides were eluted using a 120-min gradient (0 to 70% acetonitrile in 0.2 M acetic acid; 50 nl/min). Data were collected using the mass spectrometer in data-dependent acquisition mode to collect tandem mass spectra and examined using Mascot software (Matrix Science).

### Network analysis

Protein-protein and kinase-substrate interactions relevant to DNA damage signaling were hand curated from primary literature available in PubMed using initial key words: "DNA damage", "cell cycle checkpoint", "chromatin structure", "ATM/ATR", "Chk1/Chk2", and "SMC proteins" and following reference lists.

### Supplementary Material

Refer to Web version on PubMed Central for supplementary material.

### Acknowledgments

We thank H. Le for screen assistance, T.R. Jones and M. Vokes for image analysis, Matter Trunnell, IT/Systems, for computing assistance. C. Whittaker, S. Hoersch, and M. Moran, for computing and data analysis assistance; C. Reinhardt, C. Ellison, and A. Gardino, for manuscript editing; P. Filippakopoulos and S. Knapp for helpful discussions. This work was supported by NIH R01-ES15339, NIH 1-U54-CA112967-04, NIH R21-NS063917, and a Broad Institute SPARC grant to MBY; a Harvard Radiation Oncology Program Research Fellowship to MEP; a Holman Pathway Research Resident Seed Grant, American Society for Radiation Oncology Junior Faculty Career Research Training Award Klarman Scholar, and Burroughs Wellcome Career Award for Medical Scientists to SRF.

### References

1. Jackson SP, Bartek J. The DNA-damage response in human biology and disease. *Nature*. 2009; 461:1071–1078. [PubMed: 19847258]
2. Misteli T, Soutoglou E. The emerging role of nuclear architecture in DNA repair and genome maintenance. *Nat Rev Mol Cell Biol*. 2009; 10:243–254. [PubMed: 19277046]
3. Gorgoulis VG, et al. Activation of the DNA damage checkpoint and genomic instability in human precancerous lesions. *Nature*. 2005; 434:907–913. [PubMed: 15829965]

4. Bartkova J, et al. DNA damage response as a candidate anti-cancer barrier in early human tumorigenesis. *Nature*. 2005; 434:864–870. [PubMed: 15829956]
5. Kastan MB, Bartek J. Cell-cycle checkpoints and cancer. *Nature*. 2004; 432:316–323. [PubMed: 15549093]
6. Polo SE, Jackson SP. Dynamics of DNA damage response proteins at DNA breaks: a focus on protein modifications. *Genes Dev*. 2011; 25:409–433. [PubMed: 21363960]
7. Moffat J, et al. A lentiviral RNAi library for human and mouse genes applied to an arrayed viral high-content screen. *Cell*. 2006; 124:1283–1298. [PubMed: 16564017]
8. Carpenter AE, et al. CellProfiler: image analysis software for identifying and quantifying cell phenotypes. *Genome Biol*. 2006; 7:R100. [PubMed: 17076895]
9. Rahman S, et al. The Brd4 extraterminal domain confers transcription activation independent of pTEFb by recruiting multiple proteins, including NSD3. *Mol Cell Biol*. 2011; 31:2641–2652. [PubMed: 21555454]
10. Yang Z, et al. Recruitment of P-TEFb for stimulation of transcriptional elongation by the bromodomain protein Brd4. *Molecular Cell*. 2005; 19:535–545. [PubMed: 16109377]
11. Jang MK, et al. The bromodomain protein Brd4 is a positive regulatory component of P-TEFb and stimulates RNA polymerase II-dependent transcription. *Molecular Cell*. 2005; 19:523–534. [PubMed: 16109376]
12. Murga M, et al. Global chromatin compaction limits the strength of the DNA damage response. *The Journal of Cell Biology*. 2007; 178:1101–1108. [PubMed: 17893239]
13. Ziv Y, et al. Chromatin relaxation in response to DNA double-strand breaks is modulated by a novel ATM- and KAP-1 dependent pathway. *Nature*. 2006; 8:870–876.
14. Cowell IG, et al. gammaH2AX foci form preferentially in euchromatin after ionising-radiation. *PLoS ONE*. 2007; 2:e1057. [PubMed: 17957241]
15. Kim JA, Kruhlak M, Dotiwala F, Nussenzweig A, Haber JE. Heterochromatin is refractory to -H2AX modification in yeast and mammals. *The Journal of Cell Biology*. 2007; 178:209–218. [PubMed: 17635934]
16. Filippakopoulos P, et al. Histone Recognition and Large-Scale Structural Analysis of the Human Bromodomain Family. *Cell*. 2012; 149:214–231. [PubMed: 22464331]
17. Filippakopoulos P, et al. Selective inhibition of BET bromodomains. *Nature*. 2010; 468:1067–1073. [PubMed: 20871596]
18. Bradner JE, et al. Chemical phylogenetics of histone deacetylases. *Nat Chem Biol*. 2010; 6:238–243. [PubMed: 20139990]
19. Wu N, Yu H. The Smc complexes in DNA damage response. *Cell & Bioscience*. 2012; 2:5. [PubMed: 22369641]
20. Lee H-S, Park J-H, Kim S-J, Kwon S-J, Kwon J. A cooperative activation loop among SWI/SNF,  $\gamma$ -H2AX and H3 acetylation for DNA double-strand break repair. *EMBO J*. 2010; 1–12.10.1038/emboj.2010.27
21. Verhaak RGW, et al. Integrated genomic analysis identifies clinically relevant subtypes of glioblastoma characterized by abnormalities in PDGFRA, IDH1, EGFR, and NF1. *Cancer Cell*. 2010; 17:98–110. [PubMed: 20129251]
22. Carey M, Smale ST. Micrococcal Nuclease-Southern Blot Assay: I. MNase and Restriction Digestions. *CSH Protoc* 2007. 2007 pdb.prot4890.

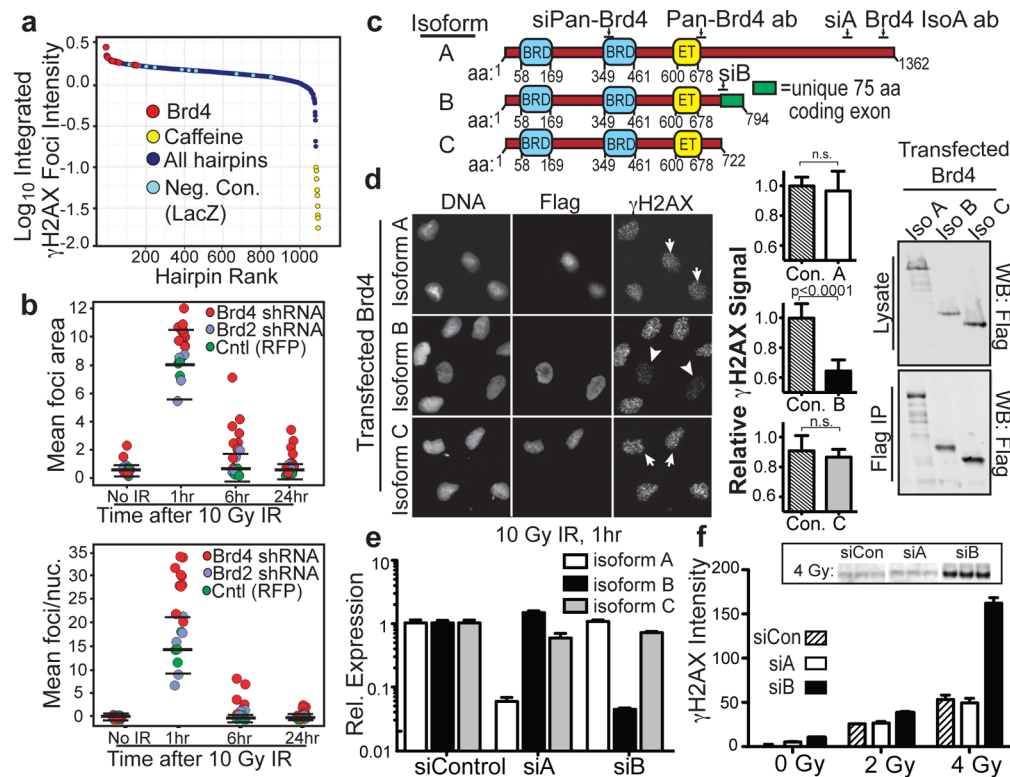


**Figure 1. Brd4 isoform B suppresses H2AX phosphorylation after ionizing radiation**

**a**, Rank of hairpins from shRNA screen ordered by integrated  $\gamma$ H2AX foci intensity at 1 hr following 10 Gy IR (details of screening assay in Supplementary Figs. 1–4). **b**,  $\gamma$ H2AX foci size (upper panel), and mean  $\gamma$ H2AX foci per nucleus (lower panel) after 10 Gy IR from cells expressing indicated shRNAs (bars show mean and 2 S.D. of control values). **c**, Domain structure of Brd4 isoforms showing conserved tandem bromodomains (BRD), extra-terminal (ET) domain, siRNA and antibody target sequences, and unique isoform B exon. **d**, H2AX phosphorylation in cells expressing FLAG-tagged Brd4 isoform B (arrowheads) or A and C (arrows) at 1 hr after 10 Gy IR. Left: representative images. Middle: quantification of 10 fields from 2 independent experiments with mean  $\gamma$ H2AX signal normalized to untransfected cells. Right: Immunoblot of isoform expression levels in whole cell lysates and anti-FLAG immunoprecipitates. **e**, Isoform-specific Brd4 knockdown in cells transfected with the indicated siRNA and analysed by quantitative real-time RT-PCR ( $n=3$ ). **f**, H2AX phosphorylation levels 1 hr after indicated IR exposure in cells transfected with isoform-specific siRNA ( $n=3$ ). Inset shows representative immunoblot for triplicate samples. Data are from U2OS cells. Error bars indicate S.E.M. and p-values were determined using Student's t-test in this and all subsequent figures unless otherwise indicated.



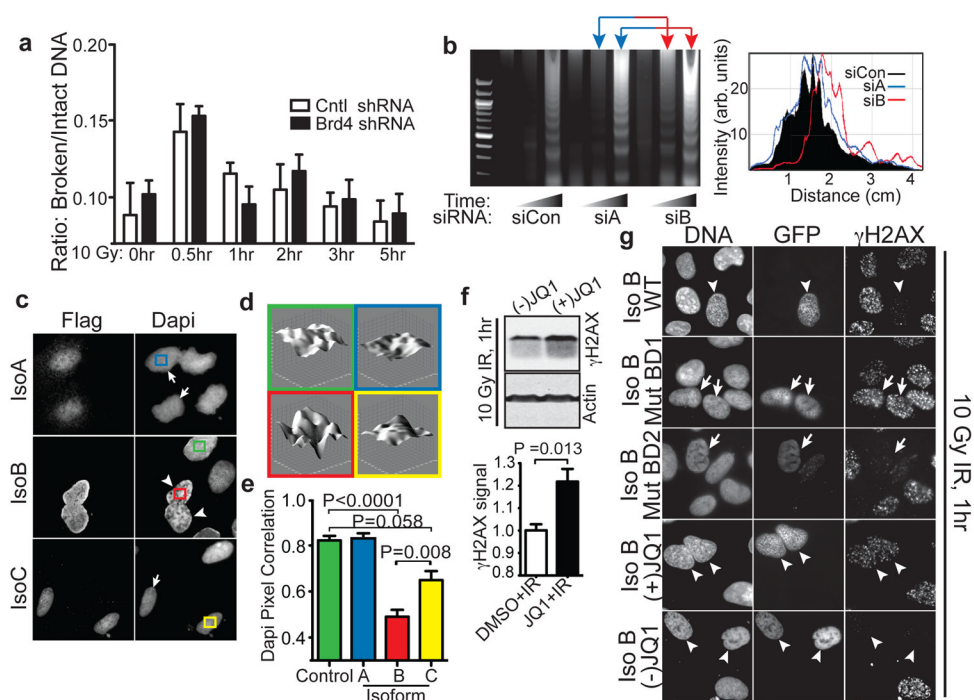


**Figure 2. Brd4 isoform B limits H2AX phosphorylation via bromodomain-acetyl lysine mediated effects on chromatin structure**

**a**, Pulsed-field electrophoresis analysis of DNA from stable cell lines expressing indicated shRNA after 10 Gy IR (n=3). **b**, Left: Micrococcal nuclease assay of control or Brd4 knockdown cells. Right: Line traces of representative gel lanes as in left panel. **c**, Chromatin structure from cells expressing FLAG-tagged Brd4 isoform B (arrowheads) or A and C (arrows) revealed by DAPI staining. **d**, 3D representation of nuclear DAPI staining intensity from cells in (c) as indicated by colored frames. **e**, DAPI pixel correlation from Brd4 isoform A, B, C and untransfected control cells (n=3). **f**, Immunoblots (upper panels) and quantification (lower panels) of H2AX phosphorylation following 250 nM DMSO, or active (+) and inactive (–) JQ1 at 1 hr after 10 Gy IR (n=3). **g**,  $\gamma$ H2AX signal 1 hr after 10 Gy IR in cells expressing GFP-wild-type Brd4 isoform B (arrowheads), isoform B with mutations that abrogate acetyl lysine binding of bromodomain 1 (BD1) or 2 (BD2) (arrows), or wild-type Brd4 isoform B in the presence of 250 nM (–) JQ1 (inactive) or (+) JQ1 as indicated.

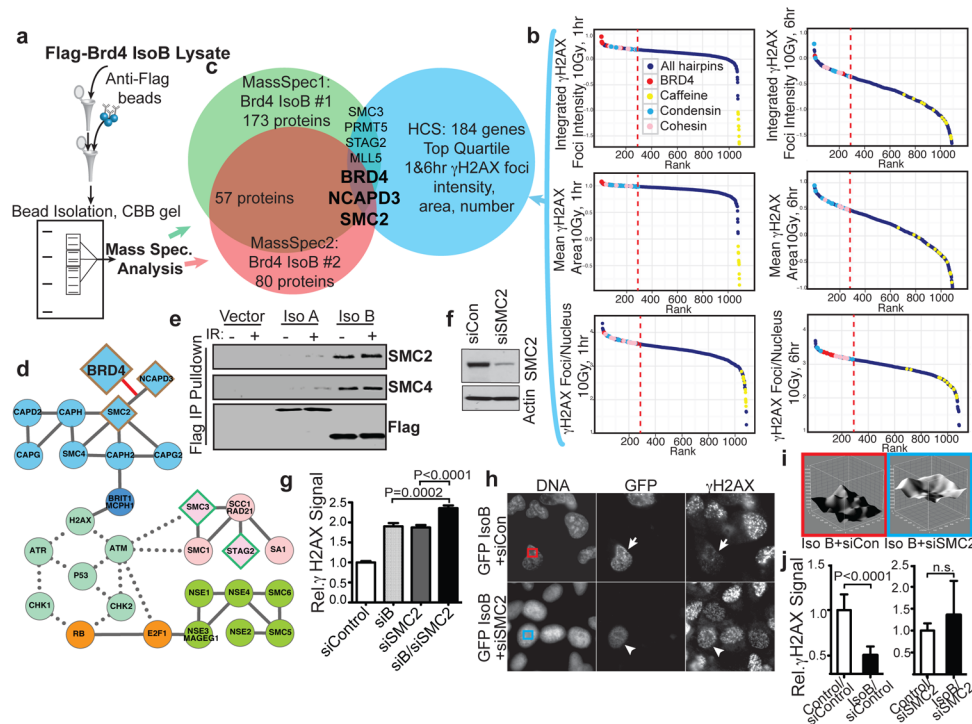


**Figure 3. Brd4 isoform B interaction with the condensin complex affects H2AX phosphorylation**  
**a**, Mass spectrometry identification of co-immunoprecipitated proteins from FLAG-tagged Brd4 isoform B-expressing cells. **b**, Identification of candidate Brd4 interactors by ranking chromatin modifier shRNAs from screen for elevated H2AX foci intensity, area and number at 1 and 6 hr after 10 Gy IR. Dashed red lines indicate top quartile. **c**, Intersection of two independent mass-spectrometry experiments (a) with the top quartile of candidates in (b). Overlapping set includes Brd4, SMC2 and NCAPD3. **d**, Network representation of SMC proteins and relationship to DNA damage signaling with protein-protein and kinase-substrate interactions collated from the literature. Protein-protein and kinase-substrate interactions shown by solid and dotted lines, respectively. Colors indicate condensin complex (blue), cohesin complex (pink), other SMC protein complexes (green), cell cycle regulators (orange) and DNA damage signaling machinery (mint). Diamonds show mass spectrometry and HCS hits from (a-b). Border colors denote overlap of screens from (c). The novel interaction of Brd4 with the condensin complex is indicated by red line. **e**, Validation of isoform B-condensin interaction with blotting immunoprecipitates from cells transfected with indicated FLAG-tagged constructs. **f**, Immunoblot verification of SMC2 knockdown from cells transfected with SMC2 siRNA. **g**, Nuclear  $\gamma$ H2AX signal from cells transfected with indicated combinations of control DNA, Brd4 isoform B, and/or SMC2 siRNA. Data was quantified from 10 fields of 2 independent experiments normalized to control cells. **h**, H2AX phosphorylation 1 hr after 10 Gy IR in cells simultaneously expressing isoform B and control (arrows) or SMC2 siRNA (arrowheads). **i**, Chromatin staining pattern in cells simultaneously expressing isoform B and control (red frame) or SMC2 (blue frame) siRNA. **j**, Mean nuclear  $\gamma$ H2AX signal in GFP-isoform B expressing cells +/- SMC2 knock-down. Data is from 10 fields of 2 independent experiments as in (h) normalized to control untransfected cells.

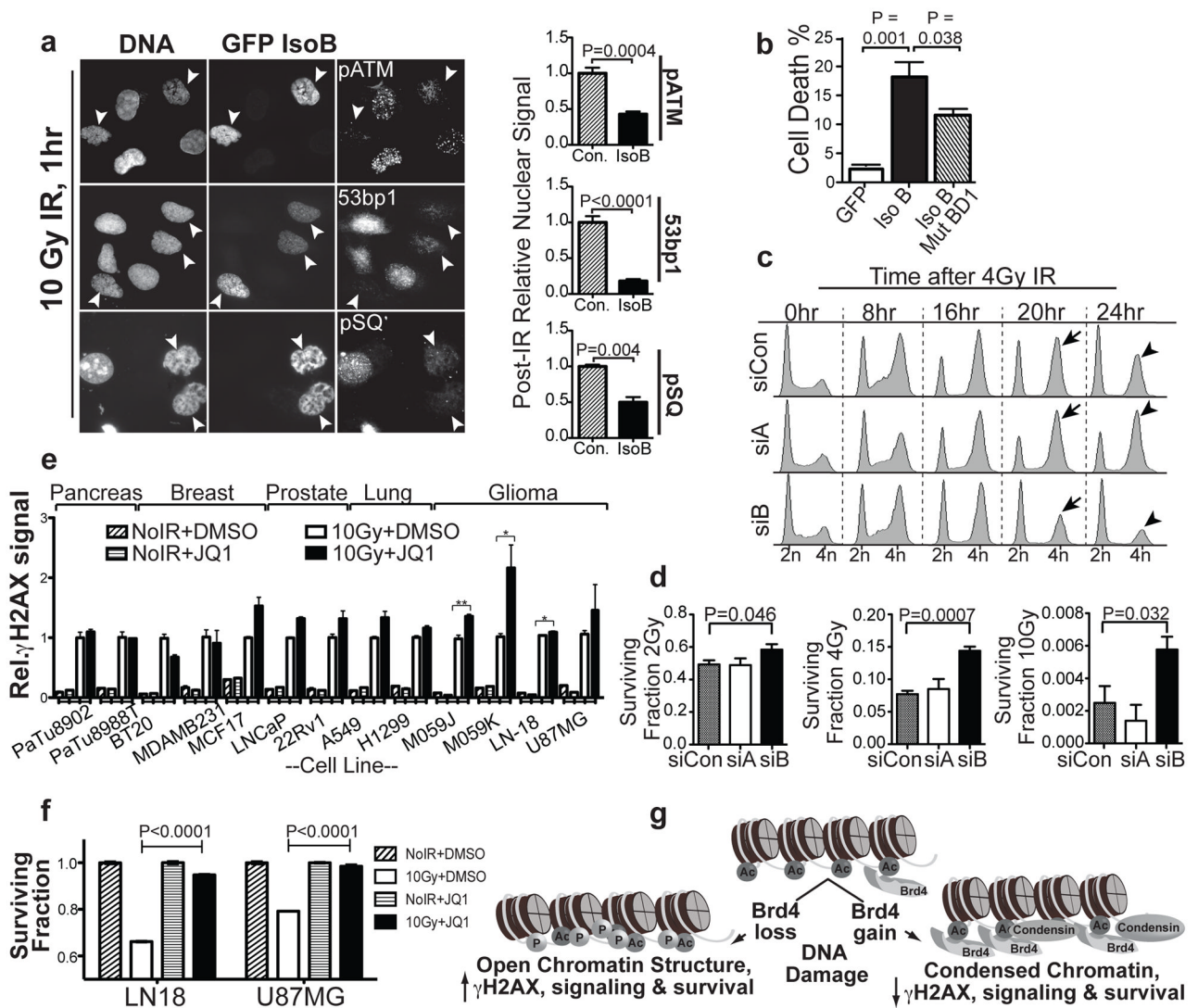


**Figure 4. Brd4 isoform B affects ionizing radiation-induced cell cycle checkpoints and survival**  
**a**, Loss of DNA damage signaling in cells expressing Brd4 isoform B. Left: representative images stained for indicated DDR proteins 1 hr after 10 Gy IR. Arrowheads indicate isoform B-expressing cells. Right: quantitation of 10 representative fields from 2 independent experiments normalized to untransfected cells. **b**, Cell death 24 hr after 10 Gy IR in cells expressing WT or bromodomain 1-mutant isoform B scored for cleaved caspase 3 by flow cytometry (n=3). **c**, IR-induced cell cycle arrest and recovery in Brd4 isoform knockdown cells assayed by propidium iodide staining and flow cytometry. **d**, Cell survival after irradiation in Brd4 isoform knockdown cells measured by colony formation. **e**, JQ1 effect on  $\gamma$ H2AX in multiple human cancer cell types commonly treated with radiotherapy. **f**, Radiation survival effects of JQ1 in glioma cell lines measured at 72 hr by CellTiterGlo (n=3). **g**, Model for Brd4 effects on DNA damage signaling.